Multivalent Rab interactions determine tether-mediated membrane fusion

Anna Lürick[a], Jieqiong Gao[a], Anne Kuhlee[b], Erdal Yavavli[a], Lars Langemeyer[a], Angela Perz[a], Stefan Raunser[b], and Christian Ungermann[a,*]

[a]Biochemistry Section, Department of Biology/Chemistry, University of Osnabrück, 49076 Osnabrück, Germany; [b]Department of Physical Biochemistry, Max-Planck Institute of Molecular Physiology; 44227 Dortmund, Germany

ABSTRACT **Membrane fusion at endomembranes requires cross-talk between Rab GTPases and tethers to drive SNARE-mediated lipid bilayer mixing. Several tethers have multiple Rab-binding sites with largely untested function. Here we dissected the lysosomal HOPS complex as a tethering complex with just two binding sites for the Rab7-like Ypt7 protein to determine their relevance for fusion. Using tethering and fusion assays combined with HOPS mutants, we show that HOPS-dependent fusion requires both Rab-binding sites, with Vps39 being the stronger Ypt7 interactor than Vps41. The intrinsic amphipathic lipid packaging sensor (ALPS) motif within HOPS Vps41, a target of the vacuolar kinase Yck3, is dispensable for tethering and fusion but can affect tethering if phosphorylated. In combination, our data demonstrate that a multivalent tethering complex uses its two Rab bindings to determine the place of SNARE assembly and thus fusion at endomembranes.**

Monitoring Editor
Benjamin S. Glick
University of Chicago

Received: Nov 7, 2016
Accepted: Nov 10, 2016

INTRODUCTION

Organelles of the endomembrane system are interconnected by vesicular transport, which delivers proteins and lipids to the right destination. Vesicle fusion with target organelles occurs in consecutive steps of Rab-dependent tethering and soluble *N*-ethylmaleimide–sensitive factor attachment protein receptor (SNARE)–mediated bilayer mixing (Kümmel and Ungermann, 2014).

Rabs are small GTPases with a C-terminal prenyl anchor, which require guanine nucleotide exchange factors (GEFs) for their membrane recruitment and GTP loading. GTP-loaded Rabs can bind effectors such as tethering factors. GTPase-activating proteins (GAPs) promote GTP hydrolysis, which enables the chaperone GDP dissociation inhibitor (GDI) to extract the Rab from membranes (Barr, 2013).

We are only beginning to understand membrane tethering at the molecular level. To address the function of long coiled-coil tethers, previous studies took advantage of in vivo targeting (Wong and Munro, 2014), in vitro systems (Drin *et al.*, 2008; Cheung *et al.*, 2015; Murray *et al.*, 2016), or cell membranes and cytosol to identify components (Cao *et al.*, 1998; Cao and Barlowe, 2000), whereas the function of multimeric tethering complexes is only partially understood. One of the best characterized multimeric tethering complexes is the vacuolar/lysosomal homotypic fusion and vacuole protein sorting (HOPS) complex (Stroupe *et al.*, 2009; Ostrowicz *et al.*, 2010; Plemel *et al.*, 2011; Balderhaar and Ungermann, 2013; Zick and Wickner, 2014). The hexameric HOPS forms an elongated and flexible tadpole-like structure (Bröcker *et al.*, 2012). The Sec1/Munc18-like Vps33 and Vps16 are located proximal to Vps41 in the large head of HOPS, whereas Vps18 and Vps11 form the link to Vps39 located at the smaller tail of HOPS (Bröcker *et al.*, 2012). Similar findings on subunit organization were made for the human HOPS complex (van der Kant *et al.*, 2015).

Based on the structural arrangement of the subunits, current data agree with a model that HOPS binds the Rab Ypt7 at its opposite ends via the subunits Vps41 and Vps39 to cluster membranes (Hickey and Wickner, 2010; Ho and Stroupe, 2015; Orr *et al.*, 2015, 2016) and thus promotes fusion by chaperoning SNARE assembly via Vps33 (Baker *et al.*, 2015). Vps33 can bind both individual SNAREs and the assembled SNARE complex to support SNARE-catalyzed fusion (Collins *et al.*, 2005; Starai *et al.*, 2008; Baker *et al.*, 2015; Lürick *et al.*, 2015).

We previously showed that HOPS is regulated in vivo by the casein kinase Yck3 (LaGrassa and Ungermann, 2005; Cabrera *et al.*, 2009, 2010). Yck3 is sorted via the AP-3 pathway from the Golgi to

This article was published online ahead of print in MBoC in Press (http://www.molbiolcell.org/cgi/doi/10.1091/mbc.E16-11-0764) on November 16, 2016.

*Address correspondence to: Christian Ungermann (cu@uos.de).

Abbreviations used: ALPS, amphipathic lipid packaging sensor; CMAC, 7-amino-4-chloromethylcoumarin; GAP, GTPase-activating protein; GDI, GDP dissociation inhibitor; GEF, guanine nucleotide exchange factor; GFP, green fluorescent protein; HOPS, homotypic fusion and vacuole protein sorting; PI-3-P, phosphoinositide-3-phosphate; SNARE, *N*-ethylmaleimide–sensitive factor attachment protein receptor.

© 2017 Lürick *et al.* This article is distributed by The American Society for Cell Biology under license from the author(s). Two months after publication it is available to the public under an Attribution–Noncommercial–Share Alike 3.0 Unported Creative Commons License (http://creativecommons.org/licenses/by-nc-sa/3.0).

"ASCB®," "The American Society for Cell Biology®," and "Molecular Biology of the Cell®" are registered trademarks of The American Society for Cell Biology.

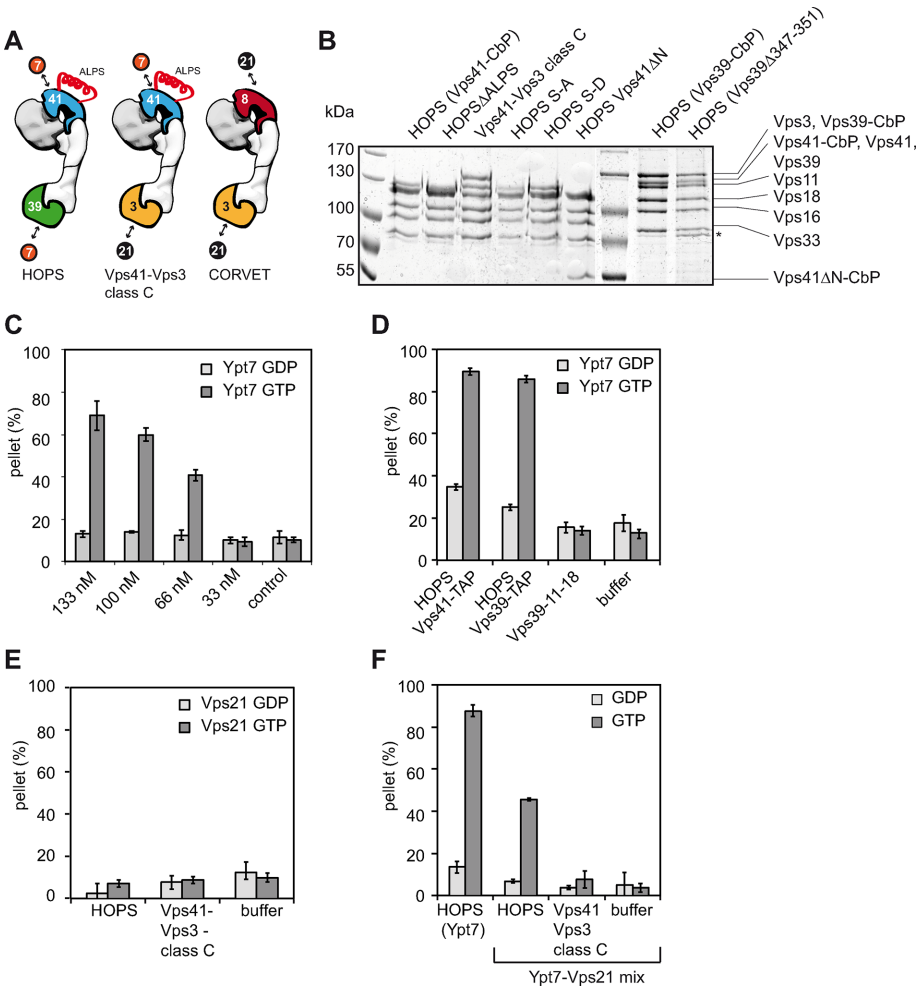

FIGURE 1: HOPS-dependent tethering is Ypt7-GTP specific. (A) Model of HOPS, CORVET, and the hybrid complex containing HOPS Vps41 and CORVET Vps3. The postulated Ypt7 (7) and Vps21 (21) binding sites are indicated. (B) Purification of different HOPS mutants. Overproduced HOPS complexes were purified from yeast via a TAP tag at the indicated subunits. Complexes were eluted from IgG-Sepharose by TEV cleavage. A 5 µg amount of each purified complex was analyzed by SDS–PAGE and Coomassie staining. The band indicated with an asterisk indicates a possible degradation product. (C, D) Wild-type HOPS tethers Ypt7-GTP–loaded liposomes. Ypt7-GDP (light gray bars) or Ypt7-GTP was targeted to liposomes by binding to the lipid analogue DOGS-NTA via their C-terminal His_6 tags (dark gray bars). For analysis, 0.170 mM Ypt7-loaded liposomes were incubated for 10 min at 27°C with increasing amounts of HOPS (C). After incubation, clustered liposomes were centrifuged at 1100 × *g* for 5 min, and the amount of liposomes in the pellet was calculated based on the signal in the supernatant. In D, 150 nM HOPS, HOPS mutant complexes, or HOPS purification buffer was used in the tethering assay. (E) HOPS is unable to tether Vps21-loaded liposomes. Liposomes were loaded with endosomal Rab GTPase Vps21-His_6 charged with either GDP (light gray) or GTP (dark gray). Assays were performed as described in C. (F) HOPS-dependent tethering decreases with the amount of Ypt7-loaded liposomes. Liposomes loaded with 0.085 mM Vps21 and 0.085 mM Ypt7 were incubated together with 90 nM tethering complex to perform tethering (indicated as Ypt7-Vps21 mix). As control, 0.170 mM Ypt7-loaded liposomes were incubated with 90 nM HOPS and analyzed for clustering (indicated as HOPS (Ypt7)). The light gray bars indicate tethering of GDP-loaded Rabs, dark gray bars of GTP-loaded Rabs. SDs are calculated from three experiments.

the vacuole and thus bypasses the endosome. At the vacuole, the kinase phosphorylates Vps41 as a prerequisite for efficient fusion of AP-3 vesicles with vacuoles (Cabrera *et al.*, 2009), yet other phosphorylation sites could not be excluded. The phosphorylation sites lie within an amphipathic lipid packing sensor (ALPS) motif of Vps41, which enables the protein to bind to highly curved membranes (Cabrera *et al.*, 2010). This suggested that nonphosphorylated HOPS recognizes small vesicles such as AP-3 vesicles or late endosomes via the ALPS motif, thus supporting the Ypt7–Vps41 interaction. In support of this idea, vacuoles purified from cells lacking Yck3 or expressing nonphosphorylatable Vps41 show partial resistance to the Ypt7 inhibitors GDI and its GAP, Gyp7 (LaGrassa and Ungermann, 2005; Brett *et al.*, 2008; Cabrera *et al.*, 2009), presumably due to a stronger interaction of Vps41 with Ypt7 and membranes (Cabrera *et al.*, 2010). When HOPS was phosphorylated by purified Yck3 in vitro or phosphomimetic mutants of Vps41 were used in vivo, membrane fusion became strongly Ypt7 dependent (Cabrera *et al.*, 2009; Zick and Wickner, 2012; Orr *et al.*, 2015). However, it was unclear whether Yck3 also acted on additional sites in HOPS that could influence tethering or fusion.

Previous studies on HOPS function in membrane tethering neither determined the function of the two Rab-binding sites in HOPS nor distinguished among multiple relevant targets of Yck3 on HOPS beyond just the ALPS motif. Here we combine mutant analyses with reconstitution assays to differentiate between tethering and fusion. We thus unravel the specific contribution of Vps41 and Vps39 to Ypt7-dependent tethering and fusion of membranes and the regulatory function of the ALPS motif.

RESULTS

Establishment of Ypt7-dependent tethering by HOPS

Within the endolysosomal pathway, the hexameric HOPS binds the Rab7-like Ypt7, whereas its endosomal cousin, the class C core vacuole/endosome tethering (CORVET) complex, interacts with the Rab5-like Vps21 (Balderhaar and Ungermann, 2013; Figure 1A). The general concept is that these tethers bridge membranes via their Rab-specific subunits (Kümmel and Ungermann, 2014).

To test this hypothesis, we focused on HOPS and initially generated multiple complexes carrying various mutations within Vps41 or Vps39. We then overproduced these complexes in yeast and purified them via C-terminal tandem affinity purification (TAP) tags on Vps41 or Vps39 (Figure 1B; discussed later; Ostrowicz *et al.*, 2010; Balderhaar *et al.*, 2013). To determine Rab-specific functions of HOPS, we modified an established liposome–liposome tethering assay (Orr *et al.*, 2015). In our system, liposomes carried a simple lipid mixture (see *Materials and Methods*) without any acidic lipids to ensure Ypt7 dependence of our assay, because HOPS cannot bind to any of these lipids (Orr *et al.*, 2015). Ypt7 with a C-terminal histidine (His) tag was preloaded with GDP or GTP before it was

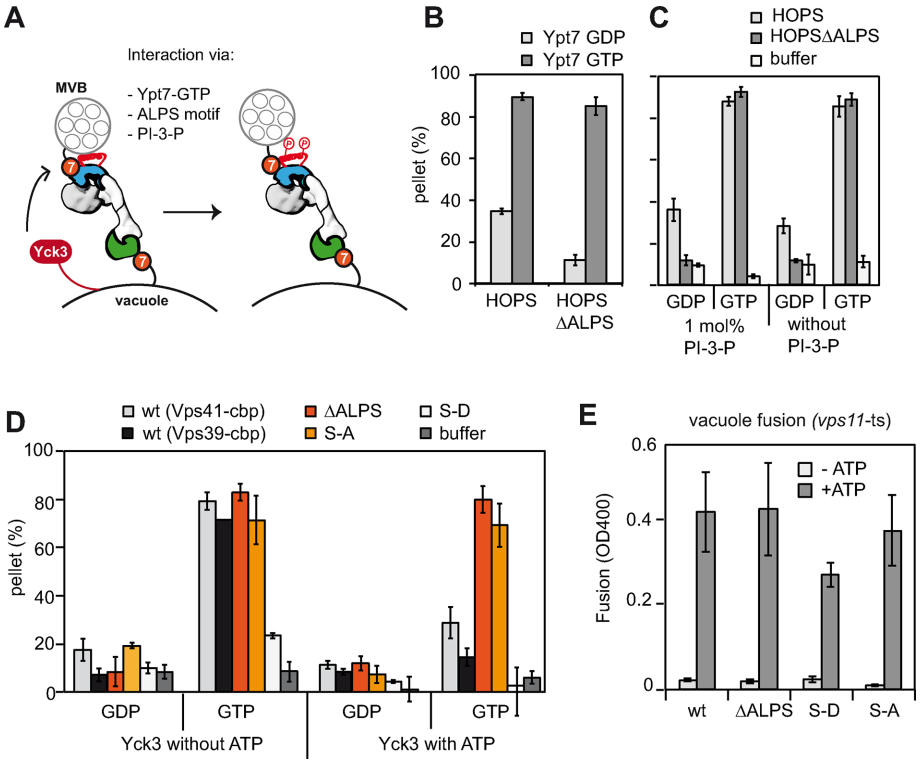

FIGURE 2: Role of the ALPS motif in HOPS for tethering. (A) Model of HOPS function in tethering. HOPS binds to Ypt7 via Vps39 (green) and Vps41 (blue). Additional membrane-binding sites exist in Vps41, which interacts with highly curved membranes via an ALPS motif and elsewhere in HOPS for PI-3-P. Yck3 can phosphorylate the ALPS motif. (B) Liposome tethering occurs in the absence of the Vps41 ALPS motif. Liposomes bearing Ypt7-GDP (light gray bars) or Ypt7-GTP (dark gray bars) were incubated with 150 nM complex and analyzed as in Figure 1C. (C) Tethering efficiency for HOPS complexes is independent of PI-3-P. Assay was performed as described in Figure 1B with the indicated liposomes. (D) Yck3 targets the ALPS motif of Vps41 and can affect tethering. We preincubated 200 nM of the different Vps41 HOPS mutants with 3 μM Yck3 and 1 mM ATP or buffer and then added them to Ypt7-loaded liposomes. Error bars are representative for three experiments. (E) Fusion activity of HOPS with mutations in the Vps41 ALPS motif. HOPS mutants were added at 100 nM to purified vacuoles purified from *vps11-ts* strains (Stroupe *et al.*, 2006; Bröcker *et al.*, 2012). Vacuoles were incubated in the absence or presence of ATP for 90 min at 26°C and then assayed for fusion. Average fusion activity obtained with each HOPS variant (three experiments).

targeted to liposomes carrying 1,2-dioleoyl-*sn*-glycero-3-[(*N*-(5-amino-1-carboxypentyl)iminodiacetic acid)succinyl] (DOGS-NTA). Tethering of liposomes was monitored by sedimentation of the liposomes in the presence of HOPS. The deviation of the liposome fluorescence signal in the supernatant before and after sedimentation was the readout for the tethering efficiency.

We initially calibrated our liposome-tethering assay for optimal Ypt7 and HOPS amounts. Liposomes had a diameter of ~100 nm and carried 3% DOGS-NTA, resulting in ~1000 binding sites for C-terminally His-tagged Ypt7 (Takamori *et al.*, 2006). The added Ypt7-His was sufficient to occupy ~1/50 of the available DOGS-NTA present in the liposomes used in each assay. When HOPS was added to Ypt7-GTP or GDP-loaded liposomes, we observed efficient tethering only with Ypt7-GTP (Figure 1C). Our titration shows that the selected amount of Ypt7 is sufficient for GTP-dependent tethering and that 133 nM HOPS did not saturate our assay. In subsequent assays, we therefore added 150 nM HOPS routinely to the tethering assay. Wild-type HOPS purified either via Vps41 or Vps39 efficiently tethered liposomes carrying Ypt7-GTP (Figure 1D) but not Ypt7-GDP or Vps21-GTP (Figure 1E). A trimeric subcomplex containing just Vps39 or a hybrid complex in which Vps39 is replaced by the CORVET subunit Vps3 (Peplowska *et al.*, 2007; Ostrowicz *et al.*, 2010) failed to tether membranes (Figure 1, D and E), although both complexes can interact with Ypt7, as revealed by pull-down analyses with Ypt7 (Ostrowicz *et al.*, 2010; Bröcker *et al.*, 2012). As a further test, we loaded liposomes with a mixture of Vps21-GTP and Ypt7-GTP and thus reduced the Ypt7 concentration on the liposomes by half. Because the used HOPS was optimized for almost-maximal tethering, a reduction of the available Ypt7 should also reduce tethering by half. We indeed obtained exactly half of the tethering efficiency, whereas the hybrid complex with just Vps41 did not tether membranes (Figure 1F). In combination, these data strongly support the concept of two Rab-binding sites within HOPS to tether membranes.

Regulation of HOPS interaction with membranes

The HOPS subunit Vps41 contains a membrane-interacting ALPS motif within its N-terminal putative β-propeller, which forms an amphipathic helix and confers binding of Vps41 to highly curved membranes (Cabrera *et al.*, 2010; Ho and Stroupe, 2015). To distinguish between a role of the ALPS motif in promoting tethering and its regulatory role due to selected phosphorylation, we generated a mutant of HOPS lacking the motif. Deletion of the Vps41 ALPS motif does not impair vacuole morphology in vivo (Cabrera *et al.*, 2010). Similarly, purified HOPS ΔALPS efficiently promoted tethering with a reproducibly stronger preference for Ypt7-GTP than the wild-type complex (Figure 2B). This indicates that, at least in the presence of Ypt7, HOPS does not require the ALPS motif to tether membranes.

HOPS has a preference to bind to phosphatidylinositol-3-phophate (PI-3-P; Stroupe *et al.*, 2006; Hickey and Wickner, 2010). We asked whether this binding preference may affect tethering, although we did not observe any noticeable difference in the presence or absence of this lipid (Figure 2C). In vivo, HOPS is required to fuse membranes of potentially high curvature, such as AP-3 vesicles, multivesicular bodies, or autophagosomes with the low-curvature vacuole (Balderhaar and Ungermann, 2013). To test whether the preference of HOPS for PI-3-P and membrane curvature via the Vps41 ALPS motif becomes critical upon tethering of membranes with strong curvature differences, we set up an assay to tether low-curvature giant unilamellar vesicles (GUVs) with liposomes of high curvature. In the presence of PI-3-P on both membranes, HOPS tethered Ypt7-positive membranes independently of the nucleotide load, whereas HOPS lacking the ALPS motif maintained its GTP preference (Figure 2 and Supplemental Figure S1A, lanes 1 and 2). To determine whether the ALPS motif on HOPS is sufficient for tethering, we omitted Ypt7 from low- or high-curvature vesicles and lost tethering (Figure 2 and Supplemental Figure S1A, lanes 3–6). Owing to the setup of the assay, we could also determine some tethering

between liposomes, which remained Ypt7 dependent under these conditions (Figure 2A and Supplemental Figure S1A, lanes 7 and 8). We then repeated the assay without PI-3-P and regained Ypt7 GTP specificity also for wild-type HOPS (Figure 2 and Supplemental Figure 1B, lanes 1 and 2). Our data thus show that tethering 1) occurs efficiently without the ALPS motif in HOPS, 2) does not require PI-3-P, and 3) cannot be achieved just via the ALPS motif if Ypt7 is lacking.

We next asked whether Yck3-mediated phosphorylation of the ALPS motif might affect tethering. We therefore analyzed HOPS complexes mimicking the nonphosphorylated (S-A) or phosphorylated (S-D) state of Vps41 in tethering, using the simpler liposome-tethering assay (Cabrera *et al.*, 2009; Figure 2D). HOPS S-A tethered liposomes in a Ypt7-GTP dependent manner as for wild-type and the ΔALPS mutant, whereas the S-D mutant showed reduced tethering (Figure 2D). To test whether the reduced tethering is due to Yck3-mediated phosphorylation, we determined tethering in the presence of purified Yck3 (Figure 2D). However, upon addition of ATP, wild-type HOPS showed strongly reduced tethering ability (light gray bars), whereas both the ΔALPS and the S-A mutant were insensitive to Yck3 addition in tethering (red and orange bars). These data are consistent with the idea that Yck3 exclusively targets the ALPS motif of Vps41 and that further phosphorylation sites do not affect HOPS function in tethering.

We had tuned our tethering assay to monitor Ypt7-dependent and HOPS-mediated tethering. To determine whether reduced tethering in this minimal system also had consequences on fusion, we used a HOPS-dependent vacuole fusion assay. We thus isolated vacuoles from a *vps11-1* temperature-sensitive strain, which have the advantage of having all regulatory factors, including the Yck3 kinase, on their surface and yet require the addition of purified HOPS for fusion (Stroupe *et al.*, 2006; Bröcker *et al.*, 2012). The fusion assay relies on the processing of an inactive enzyme present in one vacuole population with the protease containing vacuoles of the other population, and fusion activity can be detected by a simple colorimetric assay (Haas,1995). When we incubated the two tester vacuoles in the presence of ATP, wild-type HOPS restored fusion activity (Figure 2E). Both the ΔALPS and the S-A mutant complex had comparable activity to wild type, even though only wild-type HOPS is also phosphorylated during the fusion assay (Figure 2E). This shows that the ALPS motif is dispensable for both tethering and fusion. The phosphomimetic S-D HOPS had lower fusion activity, in agreement with the impaired tethering activity. HOPS mutants targeting the ALPS motif are nevertheless far more robust in fusion than in tethering, indicating that Ypt7-binding combined with additional interactions such as lipid binding can promote tethering and fusion. Yck3 thus targets exclusively the Vps41 ALPS motif and consequently regulates HOPS function rather than controls fusion.

Identification of the two Rab-binding sites in Vps41 and Vps39

Ypt7 is critical for the localization and function of HOPS in vivo (Bröcker *et al.*, 2012) and for tethering in vitro (Hickey and Wickner, 2010; Ho and Stroupe, 2015; Orr *et al.*, 2015). Even though the data presented here and previously suggest a bridging role of HOPS between membranes, the relative contribution of each Ypt7-interacting HOPS subunit and the role of the ALPS motif in membrane fusion were only deduced indirectly.

We focused on the N-terminal domains of Vps41 and Vps39 as putative Ypt7-binding sites (Ostrowicz *et al.*, 2010; Plemel *et al.*, 2011), and initially attempted to generate HOPS mutants with deletions of the entire β-propeller of Vps41 or Vps39. This was successful

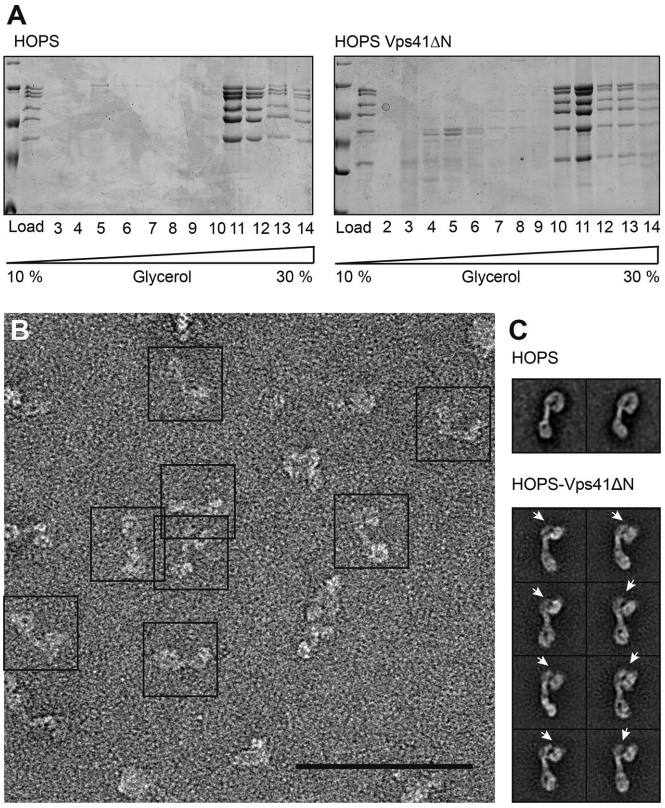

FIGURE 3: Structural analysis of the HOPS-Vps41ΔN complex by negative-stain electron microscopy. (A) HOPS with N-terminally truncated Vps41 forms a stable complex. Purified HOPS was separated on a 10–30% glycerol gradient as described in *Materials and Methods*. Each fraction was TCA precipitated and analyzed by SDS–PAGE. (B) Electron micrograph of negatively stained HOPS-Vps41ΔN. Scale bar, 100 nm. (C) Representative class sums of wild-type HOPS (Bröcker *et al.*, 2012) and HOPS-Vps41ΔN with a lack of density at the Vps41 area (indicated by an arrowhead). Each class contained 60–150 particles.

only for Vps41, named Vps41ΔN, and the complex could be purified like wild-type HOPS (Figures 1B and 3A). To determine the possible position of the β-propeller relative to the entire HOPS particle, we prepared samples for electron microscopy using mild cross-linking on glycerol gradients (see *Materials and Methods*). Class averages of multiple images of the mutant complex revealed a stable complex with a reproducible loss in staining density in the large head, proximal to the previously assigned position of Vps33 and Vps16 (Bröcker *et al.*, 2012; Figure 3B). The reduced staining was most obvious when we compared the Vps41ΔN complex with the previously characterized wild-type HOPS (Figure 3, C and D, arrowheads) and agrees with the identified position of Vps41 and the Ypt7-binding site in the head part of HOPS (Bröcker *et al.*, 2012). We thus conclude that deletion of the N-terminal domain of Vps41 does not impair the overall structure of HOPS.

To test for functionality, we deleted the N-terminal domain of Vps41 in cells, which resulted in strongly fragmented vacuoles (Figure 4, A and B). We expected that HOPS with two Rab-binding sites would localize more efficiently to vacuoles than a mutant version lacking one Rab-binding site. In agreement, green fluorescent protein (GFP)–tagged Vps41ΔN, which was added as an additional copy to wild-type cells, localized only partially to vacuoles, unlike

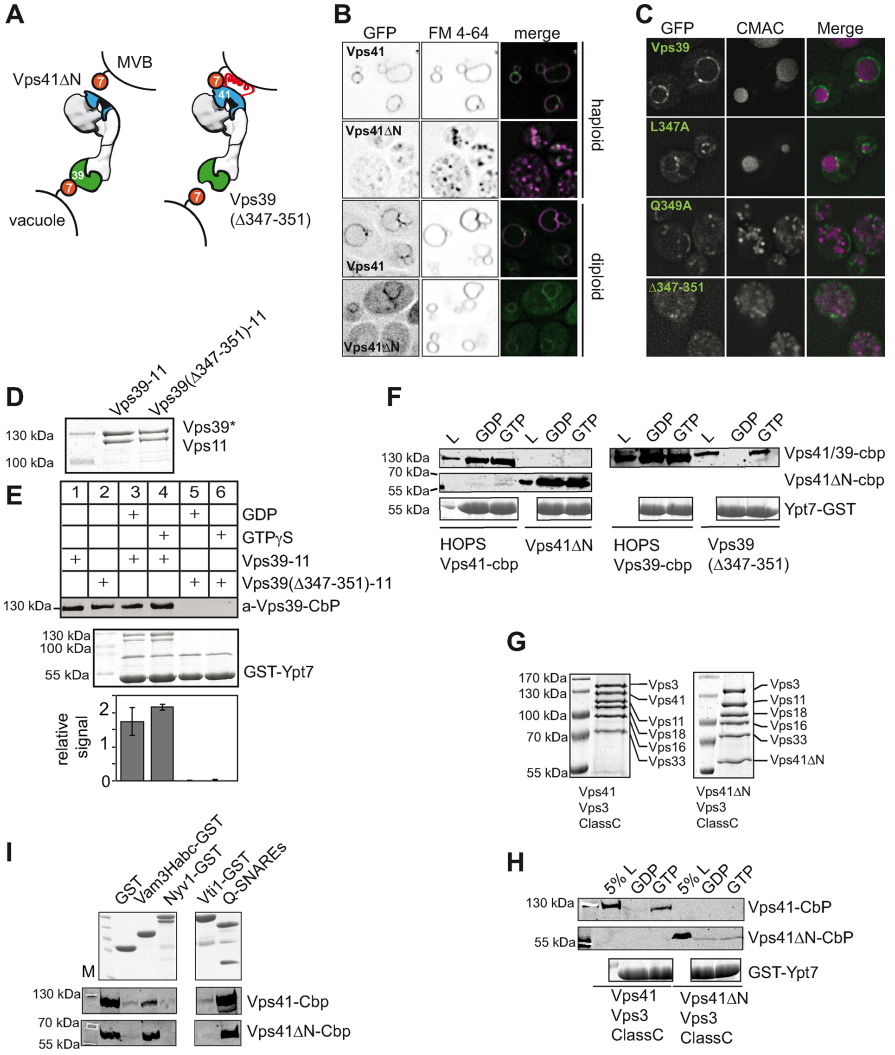

FIGURE 4: Identification of the Rab-specific recognition motifs within the two Rab-binding sites. (A) Model of Vps41 and Vps39 β-propeller mutants in tethering between MVB and vacuole. (B) Deletion of the Vps41 β-propeller disrupts the transport to the vacuole. Vps41 and Vps41ΔN were GFP tagged and analyzed in haploid or diploid yeast cells. To determine vacuole morphology in the strains, cells were stained with the lipophilic dye FM4-64 (bar, 5 μm). (C) Identification of Vps39 mutants that affect vacuole morphology. Plasmids encoding Vps39-GFP with the indicated mutations integrated into *vps39*Δ cells and stained with FM4-64. (D) Purification of Vps39-Vps11 subcomplexes from yeast. Wild-type and mutant Vps39 were co-overproduced with Vps11, purified like HOPS, and analyzed by SDS–PAGE and Coomassie staining. (E) Interaction of Vps39-Vps11 complexes with Ypt7. GST-Rabs were loaded with GTP or GDP, immobilized on GSH beads, and incubated with purified Vps39-Vps11 complexes. Eluted proteins were analyzed by Western blot with antibodies to the CbP tag (top). A fraction of the beads were boiled in sample buffer and stained with Coomassie (bottom). Load (L) equals 10% of input. (F) HOPS β-propeller mutants interact with Ypt7. A 150-μg amount of GST-Ypt7 was preloaded with the respective nucleotides and then added to GSH beads and used for pull-down assays with 30 μg of indicated complexes. Proteins were eluted as described in *Materials and Methods* and analyzed by Western blotting using anti-CbP antibody for Vps41, Vps41ΔN, or Vps39 detection (top and middle). To visualize the Ypt7 loading on GSH beads, beads were boiled, and 20% were loaded to SDS–PAGE for analysis (bottom). Load (L) equals 10% of input. (G) Purification of the hybrid hexameric complexes. Vps41-Vps3-Class C complexes with and without the N-terminal part of Vps41 were purified as in Figure 1B via the TAP tag. (H) Interaction of HOPS via Vps41 with Ypt7. Vps41-Vps3-class C complexes were subjected to Rab pull downs and analyzed as in C. (I) Interaction of HOPS Vps41ΔN with SNAREs. A 100-μg amount of GST-tagged SNAREs or a Q-SNARE complex (30 μg of GST-Vam7 SNARE domain, 80 μg of His_6-Vti1, and 80 μg of His_6-Vam3 SNARE domain) was coupled to GSH beads and incubated for 2 h at 4°C with 30 μg wild-type HOPS or HOPS Vps41ΔN. Proteins were eluted by boiling, and 80% were analyzed by Western blotting against the CbP tag of Vps41 (middle and bottom), and 20% were analyzed by SDS–PAGE (top). M, molecular weight marker.

the corresponding wild-type protein. This indicates that the N-terminal domain of Vps41 is required for HOPS localization and function in vivo.

To identify the Ypt7-binding site in Vps39, we performed alanine scanning mutagenesis of prominent charged and hydrophobic residues of the N-terminal domain, which was previously suggested as the Ypt7-binding site (Wurmser *et al.*, 2000; Plemel *et al.*, 2011), and determined localization of the respective GFP-tagged proteins and vacuole morphology (Figure 4C). Mutants targeting residues 347–351, which are located in a conserved site of the putative β-propeller, left Vps39 cytosolic and resulted in vacuole fragmentation (Figure 4C).

To test whether this site is indeed involved in Ypt7 binding, we copurified wild-type Vps39 and a mutant (Δ347–351) together with its direct binding partner, Vps11 (Figure 4D; Ostrowicz *et al.*, 2010; Bröcker *et al.*, 2012). The Vps39-11 complexes were then added to GST-Ypt7 charged with either GDP or GTP, which was immobilized to glutathione Sepharose beads (Figure 4E). We observed efficient interaction of Ypt7 with the wild-type Vps39-11 complex, whereas the mutant complex did not bind. Of note, Vps39-11 could also bind to Ypt7-GDP, due presumably to the high affinity of Vps39 for Ypt7. The mapping of the Ypt7-binding sites to the N-termini of Vps41 and Vps39 agrees with our structural analyses (Bröcker *et al.*, 2012) and previous mapping approaches (Ostrowicz *et al.*, 2010; Plemel *et al.*, 2011).

To further characterize the mutation in the context of HOPS, we incorporated the mutations into our overexpression strain and purified the corresponding HOPS complex via the modified subunit. For comparison, we used the corresponding wild-type HOPS purified via Vps39 or Vps41. We then determined SNARE and Rab interactions by glutathione *S*-transferase (GST) pull-down assays (Figure 4, F, H, and I). Because Vps41 is located proximal to the SNARE-interacting Vps33 subunit (Bröcker *et al.*, 2012), we confirm that the loss of the N-terminal domain did not impair SNARE binding. We therefore performed a pull down with assembled Q-SNAREs or the Vam3 H_{abc} domain (Lürick *et al.*, 2015) but observed no difference from wild-type HOPS (Figure 4I). We next determined the interaction of HOPS with Ypt7. HOPS with Vps41ΔN interacted as efficiently with Ypt7-GDP and Ypt7-GTP as wild-type HOPS. Because Vps39 is still present in both wild-type and mutant complexes, we conclude that this interaction is

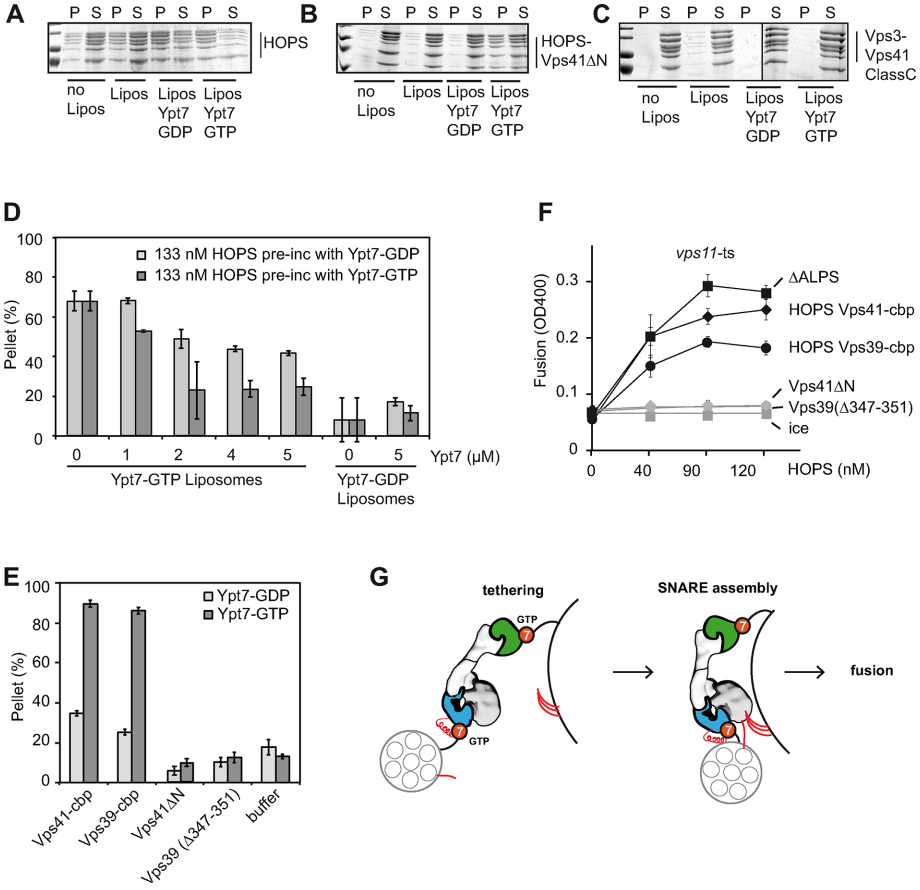

FIGURE 5: HOPS-mediated fusion requires two Rab-binding sites but not the Vps41 ALPS motif. (A–C) Association of HOPS and HOPS mutants with liposomes. Purified complexes were incubated for 10 min at 27°C without or with liposomes carrying DOGS-NTA and, where indicated, Ypt7-GTP or GDP. Reactions were then centrifuged (30 min, 20,000 × *g*, 4°C), the supernatant was removed, and proteins were TCA precipitated. Eighty percent of the pellet and supernatant fractions were solubilized in SDS sample buffer and analyzed by SDS–PAGE and Coomassie staining. (D) Effect of Ypt7 on HOPS-mediated tethering. HOPS was preincubated for 10 min at 27°C with untagged Ypt7-GTP or GDP at the indicated final concentrations. The mixture was then added to liposomes carrying His-tagged Ypt7-GTP or GDP, incubated for an additional 10 min at 27°C, and then processed as in Figure 1C. (E) Liposome tethering via HOPS mutants that lack one Ypt7-binding site. Ypt7-containing liposomes were incubated with 200 nM of each purified complex before they were pelleted by a 1100 × *g* spin. The amount of clustered liposomes was calculated. (F) Fusion activity of HOPS β-propeller mutants. The indicated HOPS mutants were applied at increasing concentrations to purified vacuoles. SDs are representative for three experiments. (G) Model of HOPS-mediated tethering and fusion.

due to the strong binding of the Vps39 subunit to Ypt7 (Figure 4F). In contrast, the interaction of HOPS containing mutated Vps39 (Δ347–351) with Ypt7 was both reduced and much more GTP specific (Figure 4F). To analyze whether this Ypt7 interaction indeed occurred via Vps41, we purified the hybrid complex containing Vps41 and the CORVET subunit Vps3, thus carrying only one Ypt7-binding site (Figure 1A; Peplowska *et al.*, 2007; Ostrowicz *et al.*, 2010). As expected, this purified hexameric complex (Figure 4G) interacted exclusively with Ypt7-GTP (Figure 4H), in agreement with our observations on HOPS with mutated Vps39 (Figure 4F). However, when we generated and purified a hybrid HOPS complex lacking the N-terminal domain of Vps41, binding to Ypt7 was entirely lost (Figure 4, G and H). Overall our data show that Vps41 binds Ypt7 via its N-terminal domain less strongly but with higher nucleotide specificity than Vps39.

Cooperation of the two Rab-binding sites is essential for HOPS function

Rab pull-down analyses have the advantage of determining interactions, although they do not necessarily reveal the relative affinity of Rabs and tethers in the context of membranes. We therefore used our mutant complexes to determine Ypt7-dependent membrane binding. For this, we incubated HOPS with liposomes in the absence and presence of Ypt7 to monitor just the membrane association rather than liposome tethering and determined the fraction of HOPS in pellet and supernatant after centrifugation. Wild-type HOPS remained largely soluble without Ypt7 on liposomes (Figure 5A). When liposomes with bound Ypt7-GDP or GTP were used, most of the HOPS was found in the pellet fraction, in agreement with the interaction of HOPS with Ypt7 by GST pull down (Figure 4F). Because HOPS has two Rab-binding sites, we used our mutant complexes to determine the contribution of Vps39 (with the Vps41ΔN complex) or Vps41 (with the hybrid complex with Vps3). We preferred the latter complex for this analysis due to its much more efficient purification and better handling. With the Vps41ΔN complex, binding to liposomes was now only observed when Ypt7-GTP was present (Figure 5B), in contrast to the binding to Ypt7-GDP and GTP by Rab pull down (Figure 4G). Binding of the Vps41-Vps3-class C hybrid complex to liposomes was close to background even in the presence of Ypt7-GTP (Figure 5C), reflecting either lower affinity of Vps41 for Ypt7 or altered behavior of the complex in the presence of membranes. Vps39 thus has a preference for Ypt7-GTP in the context of membranes.

To estimate the relative strength of the interaction between HOPS and Ypt7 in the context of membranes, we used our tethering assay. HOPS was incubated with increasing amounts of Ypt7 before being added to the tethering reaction. Without Ypt7 addition, HOPS-dependent tethering was strongly Ypt7 GTP dependent, as shown before. A fivefold excess of soluble Ypt7-GTP (2 μM) over membrane-bound Ypt7 strongly inhibited HOPS-dependent tethering (Figure 5D). Under the same conditions, Ypt7-GDP was reproducibly less inhibitory, in agreement with a strong preference of HOPS for Ypt7-GTP. The relative affinity of HOPS for Ypt7 analyzed under these minimal conditions is thus in the low-micromolar range.

Based on our analyses, the impairment of either Rab-binding site should disable HOPS in tethering and fusion. Indeed, both the Vps41ΔN complex and the complex with mutant Vps39 were entirely inactive in tethering (Figure 5E).

To compare the different mutants in fusion, we titrated HOPS to tester vacuoles from *vps11-1* cells in the presence of ATP. HOPS complexes purified via Vps41 or Vps39-TAP, as well as the HOPSΔALPS, which we used for comparison, restored fusion activity

of vacuoles (Figure 5F). As previously noted, C-terminal tagging of Vps39 resulted in lower HOPS activity (Bröcker *et al.*, 2012; Figure 5E). Of importance, both HOPS variants carrying mutations in the Ypt7-binding site were entirely unable to rescue fusion at any tested concentration (Figure 5F). We therefore conclude that both Rab-binding sites in Vps41 and Vps39 are essential in the context of the HOPS complex for function.

DISCUSSION

Our data provide strong evidence that HOPS bridges membranes via its two Rab-binding sites in Vps41 and Vps39 (Figure 5G). If either site does not recognize Ypt7 in the right context, fusion fails, even though the complex retains its ability to bind to both SNAREs and to Ypt7 via the remaining binding site. The most straightforward explanation is that HOPS needs to bridge two Ypt7-positive membranes to promote SNARE assembly via its integral Sec 1/Munc18-like Vps33 subunit. Subsequently SNAREs drive fusion exactly at the position of HOPS-mediated tethering. Thus HOPS is a position-specific membrane fusion factor that combines position recognition with SNARE chaperoning. HOPS may be representative of how tethering complexes cooperate in general with Rabs and SNAREs at endomembranes.

Several studies addressed tethering via HOPS using a variety of approaches, such as visual analysis of clustering of vacuoles, small and large liposomes, or liposome sedimentation (Wang *et al.*, 2003; Hickey and Wickner, 2010; Ho and Stroupe, 2015; Orr *et al.*, 2015). Although these studies agree with the bridging of Ypt7-decorated membranes, the direct involvement of the Rab-specific subunits was not addressed. A recent study that was published while this work was under review showed that a HOPS complex lacking Vps39 fails to tether Ypt7-decorated liposomes (Ho and Stroupe, 2016). Although we agree with the general conclusion, our study extends this by identifying both Rab-binding domains in HOPS, their relative affinity for Ypt7, and their role in fusion. We demonstrate that the HOPS complex has Ypt7-binding sites in the N-terminal predicted β-propeller domains of Vps41 and Vps39. These sites differ in their relative preference for Ypt7. The Vps41 site binds exclusively to Ypt7-GTP, although this seems to be weaker than the Vps39 site. The binding via Vps39 was also specific for Ypt7-GTP, which was most apparent, when we monitored the association of the Vps41ΔN complex with Ypt7-GTP–containing liposomes (Figure 5B). It is likely that the reduced nucleotide specificity observed in the Rab pull-down assay is a result of the stronger interaction of Vps39 with Ypt7. We believe that HOPS will only see Ypt7-GTP in vivo, as GEF-mediated activation of Ypt7 and GDI will control the nucleotide status of Ypt7 (Nordmann *et al.*, 2010; Bröcker *et al.*, 2012; Auffarth *et al.*, 2014).

Using the tethering assay, we also addressed the affinity of HOPS for Ypt7 by titrating soluble Ypt7 to the assay. The low-micromolar affinity agrees with previously described affinities between Rabs and their effectors (Eathiraj *et al.*, 2005; Burguete *et al.*, 2008; Mishra *et al.*, 2010; Vetter *et al.*, 2015; Rai *et al.*, 2016). This membrane affinity of HOPS for Ypt7 is likely higher when it occurs in the context of membranes, as acidic lipids promote membrane association of HOPS in vitro (Orr *et al.*, 2015).

Why does HOPS have two binding sites with different affinity for the same Rab? Rab binding will not necessarily position HOPS perpendicular to the membranes, but it may allow its engagement with two Rabs on the same membrane. The asymmetric affinity of the two Ypt7-binding sites allows HOPS to bind to vacuoles continuously via Vps39 while more easily releasing Ypt7 at the Vps41 site, possibly supported by phosphorylation of the ALPS motif (Cabrera *et al.*, 2010). This will be important in order to recognize Ypt7 present on late endosomes before their fusion with vacuoles (Figure 5H). In our view, the HOPS ALPS motif is a regulatory motif to support tethering via Vps41 and make Vps41 available again after fusion. It indeed binds highly curved vesicles (Cabrera *et al.*, 2010) and thus promotes tethering (Ho and Stroupe, 2016). With less-curved vesicles, we did not observe ALPS-dependent tethering in the absence of Ypt7, and HOPS lacking the motif promoted fusion like wild-type HOPS (this study). HOPS thus does not need this motif for functionality. If present, it can be phosphorylated by Yck3, which lowers tethering efficiency in vitro (Figure 2; Hickey and Wickner, 2010; Ho and Stroupe, 2015; Orr *et al.*, 2015) but not Ypt7-dependent fusion of vacuoles (Figure 5F). Because Yck3 mutants and mutations within the Vps41 ALPS motif that remove the phosphorylation sites selectively impair the AP-3 pathway but neither vacuole fusion nor any other trafficking routes (Anand *et al.*, 2009; Cabrera *et al.*, 2009), we consider it likely that this kinase primarily modulates HOPS on vacuoles to make Vps41 available for the AP-3 pathway.

As implied by our structural analysis of HOPS (Bröcker *et al.*, 2012; Lürick *et al.*, 2015), tethers such as HOPS use Rab binding to bridge membranes and confer SNARE assembly by recognizing both individual SNAREs and SNARE complexes (Jun *et al.*, 2006; Stroupe *et al.*, 2006; Lobingier *et al.*, 2014; Baker *et al.*, 2015; Lürick *et al.*, 2015). Similar interactions between Rab-binding tethers and Sec1/Munc18 proteins are known for the exocyst (Morgera *et al.*, 2011) and may apply to other tethering complexes as well. Similarly, the EEA1-like coiled-coil tether Vac1 interacts with the Sec1/Munc18 Vps45 (Tall *et al.*, 1999), and EEA1 and hVps45 cooperate to promote efficient endosome fusion (Ohya *et al.*, 2009). Of importance, our data imply that HOPS is a molecular machine by which tethering via two Rab-binding sites optimally positions the SNARE-chaperoning Vps33 to promote SNARE-driven membrane fusion.

MATERIALS AND METHODS

Strains and plasmids

Yeast strains to prepare HOPS mutants are listed in Table 1. In general, plasmids encoding the mutant Vps41 and Vps39 proteins under the control of the *GAL1* promoter were generated by site-directed mutagenesis and inserted into the genome of the HOPS-overexpression strain lacking the respective mutated protein. The respective *VPS41* and *VPS39* alleles were then C-terminally tagged with the TAP tag to ensure purification of mutant HOPS complex. Plasmids used for generation of recombinant Ypt7 and SNAREs have been described (Cabrera *et al.*, 2014; Lürick *et al.*, 2015).

Tandem affinity purification

Cells expressing HOPS or HOPS mutants were grown to an OD_{600} of 12, centrifuged for 5 min at 5000 × *g*, and resuspended in TAP buffer (300 mM NaCl, 50 mM 4-(2-hydroxyethyl)-1-piperazineethanesulfonic acid [HEPES]/NaOH, pH 7.5, 1.5 mM $MgCl_2$, 1 mM dithiothreitol [DTT], 1 mM phenylmethylsulfonyl fluoride [PMSF], and 1× FY protease inhibitor mix [Serva], 10% glycerol). Lysis was performed in a Disrupter Genie three times for 10 min in the presence of glass beads. Beads were removed by centrifugation at 3000 × *g* for 20 min at 4°C. The supernatant was centrifuged for 1 h at 100,000 × g. Then the clear lysate was incubated with 300 µl of prewashed immunoglobulin G (IgG) beads (GE Healthcare) for 2 h at 4°C. Beads were washed with 15 ml of TAP buffer without PMSF and FY. Proteins were eluted from IgG beads by TEV protease treatment for 1 h at 16°C.

Strain	Genotype	Reference
BY4727	MAT*alpha his3Δ200 leu2Δ0 met15Δ0 trp1Δ63 ura3Δ200 leu2Δ0 met15Δ0 trp1Δ63 ura3Δ0*	Brachmann *et al.*, 1998
BY4732	MAT*a his3Δ200 met15Δ0 trp1Δ63 ura3Δ0*	Brachmann *et al.*, 1998
BY4741	MAT*a his3Δ1 leu2Δ0 met15Δ0 ura3Δ0*	Brachmann *et al.*, 1998
CUY1953	BY4732 *VPS41::TRP1-GAL1pr VPS41::TAP-URA3 VPS39::KanMX-GAL1pr VPS33::HIS3-Gal1pr*	Ostrowicz *et al.*, 2010
CUY2489	BY4727 *VPS11::HIS3-GAL1Pr VPS16::natNT2-GAL1Pr VPS18::kanMX-GAL1Pr-3HA*	Ostrowicz *et al.*, 2010
CUY2675	CUY1953xCUY2489	Ostrowicz *et al.*, 2010
CUY3396	BY4727 *VPS11::HIS3-GAL VPS39::CloNat-GAL VPS39::TAP-URA3 VPS18::TRP1-GAL1*	Bröcker *et al.*, 2012
CUY3799	BY4732 *VPS39::KanMX-Gal1Pr VPS33::HIS3-GAL1pr GAL1pr::pRS406-GAL1pr-VPS41(356-379Δ)-URA3 VPS41::TAP-TRP*	This study
CUY3802	CUY2489xCUY3799	This study
CUY4605	CUY4640xCUY4641	This study
CUY4640	BY4727 *VPS11::HIS3-GAL1pr VPS16::natNT2-GAL1pr VPS18::kanMX-GAL1pr-3HA VPS33::TRP1-GAL1pr*	This study
CUY4641	BY4741 *VPS3::kanMX-Gal1pr VPS41::NatNT2-GAL1pr VPS41::TAP-URA3*	This study
CUY5659	BY4732 *VPS39::KanMX-Gal1Pr VPS33::HIS3-GAL1pr GAL1pr::pRS406-GAL1pr-Vps41 S-A-URA3 VPS41 S-A::TAP-TRP1*	This study
CUY5666	CUY5659xCUY2489	This study
CUY8078	BY4732 *VPS39::KanMX-Gal1Pr VPS33::HIS3-GAL1pr GAL1pr::pRS406-Gal1pr-VPS41 S-D-URA3 VPS41 S-D::TAP-TRP1*	This study
CUY8243	CUY8078xCUY2489	
CUY8292	BY4727 *VPS11::HIS3-GAL1pr VPS16::natNT2-GAL1pr VPS18::kanMX-GAL1pr-3HA vps41Δ::hphNT1*	This study
CUY8356	BY4732 *VPS39::KanMX-Gal1pr VPS33::HIS3-GAL1pr VPS41(1-499Δ)::CloNAT-GAL1pr vps41Δaa1-499-TAP::URA*	This study
CUY8367	CUY8356xCUY8292	This study
CUY10111	BY4732 *VPS41::TRP1-GAL1pr VPS33::HIS3-GAL1pr GALpr::pRS406-GALpr-VPS39(347-351Δ)-TAP-URA3*	This study
CUY10122	CUY10111xCUY2489	This study
CUY10153	BY4732 *VPS41::TRP1-GAL1pr VPS33::HIS3-GAL1pr GAL::pRS406-GAL1pr-VPS39-TAP*	This study
CUY10154	CUY10153xCUY2489	This study
CUY10043	BY4727 *vps39Δ::hphNT1 NOP1::pRS406-NOP1pr-VPS39-GFP*	This study
CUY10045	BY4727 *vps39Δ::hphNT1 NOP1pr::pRS406-NOP1pr-VPS39(L347A)-GFP*	This study
CUY10046	BY4727 *vps39Δ::hphNT1 NOP1::pRS406-NOP1pr-VPS39(Q349A)-GFP*	This study
CUY10056	BY4727 *vps39Δ::hphNT1 NOP1::pRS406-NOP1pr-VPS39(347-351Δ)-GFP*	This study
CUY10054	BY4727 *vps11::HIS3-GAL URA3::pRS406-GAL1pr-Vps39-TAP*	This study
CUY10155	BY4727 *vps11::HIS3-GAL GAL::pRS406-GAL1pr-VPS39(347-351Δ)-TAP*	This study
CUY10385	CUY4605 *VPS41(1-499Δ)::hphNT1-GAL1pr*	This study
CSY9	*vps11Δ::HIS3MX6 pep4Δ::KanMX6 VPS11-1ts-URA3*	Stroupe *et al.*, 2006
CSY10	*vps11Δ::HIS3MX6 pho8Δ::KanMX6 VPS11-1ts-URA3*	Stroupe *et al.*, 2006

TABLE 1: Strains used in this study.

Escherichia coli protein expression and purification

SNARE proteins and Rab GTPases used for pull-down or tethering assays were expressed in *Escherichia coli* BL21 (DE3) Rosetta cells. Cells grown in Luria broth (LB) medium supplemented with the specific antibiotics had been induced at $OD_{600} = 0.4$ with 0.75 mM isopropyl-β-D-thiogalactoside overnight at 16°C. Harvested cells were lysed by a Microfluidizer Processor M-110L (Microfluidics) in buffer containing 150 mM NaCl, 50 mM HEPES/NaOH, pH 7.5, 1 mM PMSF, and 0.5-fold protease inhibitor mixture. For Rab GTPase purification, the buffer concentration was reduced to 20 mM HEPES/NaOH. After centrifugation of the lysates for 20 min at 25,000 × *g*, the supernatants were incubated with glutathione-Sepharose (GSH) fast flow beads (GE-Healthcare) for 1 h at 4°C for GST-tagged proteins or nickel–nitriloacetic acid (Ni-NTA) agarose (Qiagen) for His-tagged proteins. Ni-NTA beads were washed with 25 ml of lysis buffer lacking PMSF and protease

inhibitor mixture but containing 20 mM imidazole. The same buffer was used for elution with an increased imidazole concentration of 0.3 M imidazole. GST-tagged proteins were eluted with a buffer containing 15 mM glutathione. After elution, the buffer was exchanged via a PD10 column (GE Healthcare) containing 10% glycerol and no imidazole or glutathione. All proteins were stored at −80°C.

Rab-loading and -binding assay

Before Rab proteins were used for pull-down or tethering assays, they were loaded specifically with nucleotides (GTPγS, GTP or GDP). A 150-µg amount of Rab protein was incubated in 500 µl of nucleotide loading buffer (20 mM HEPES/NaOH, pH 7.4, 20 mM EDTA, 1 mM GTPγS, GTP, or GDP) for 30 min at 30°C on a turning wheel before the reaction was stopped with 25 mM $MgCl_2$. For pull-down assays, nucleotide-loaded, GST-tagged Rab proteins were added to 40 µl of prewashed GSH fast flow beads (GE-Healthcare), followed by 1-h incubation at 4°C. Rab-loaded GSH beads were washed three times with TAP purification buffer (300 mM NaCl, 50 mM HEPES/NaOH, pH 7.5, 1.5 mM $MgCl_2$, 1 mM DTT, 1 mM PMSF, 1× FY protease inhibitor mix [Serva], and 10% glycerol). A 25-µg amount of prey protein was added to the immobilized Rab protein and incubated for another 2 h at 4°C on a turning wheel. After the binding reaction, GSH beads were carefully pelleted and washed three times with 1 ml of cold TAP buffer. Elution of prey protein occurred by incubation for 20 min at room temperature with 600 µl of elution buffer (300 mM NaCl, 50 mM HEPES/KOH, pH 7.4, 0.1% Igepal, 1.5 mM, and 20 mM EDTA). A second elution step in 300 µl of buffer was performed to elute the residual protein. The two eluates were pooled, trichloroacetic acid (TCA) precipitated, and analyzed by SDS–PAGE and Western blot.

SNARE-binding experiments

A 100-µg amount of bait proteins (GST tagged) was coupled to 50 µl of prewashed GSH slurry and incubated at 4°C for 2 h. After incubation, slurry was washed four times with buffer (300 mM NaCl, 50 mM HEPES/NaOH, pH 7.4, 1 mM DTT, 0.15% Igepal) before 25–30 µg of prey proteins was added. For the Q-SNARE complex formation, 30 µg of GST-tagged SNARE was assembled with 80 µg of His_6-tagged SNAREs for 1 h at 4°C before they were added to the GSH slurry as bait protein. Bait and prey proteins were incubated for 1 h at 4°C, followed by a 4× washing step as mentioned earlier. Proteins were eluted from GSH slurry by boiling in 50 µl of 4× loading dye for 5 min. For analysis, 20% of eluate was used for Coomassie staining and 80% for Western blotting against the calmodulin-binding peptide (CbP) tag.

Vacuole fusion assay

Vacuoles were purified from two different tester strains—CSY9 Vps11-1ts (*pep4*Δ) and CSY10 Vps11-1ts (*pho8*Δ)—and harvested from a Ficoll gradient as described (Haas, 1995). Vacuoles were diluted to 0.3 mg/ml with 0% Ficoll (10 mM 1,4-piperazinediethanesulfonic acid [PIPES]/KOH, pH 6.8, 200 mM sorbitol, 0.1× protease inhibitor mixture [PIC]). A standard fusion reaction contained 3 µg of BJ and DKY vacuoles incubated for 90 min at 26°C in fusion buffer (125 mM KCl, 5 mM $MgCl_2$, 20 mM sorbitol, 1 mM PIPES/KOH, pH 6.8) with 10 µM CoA and 0.01 µg of His_6-Sec18. Depending on the different reactions, the fusion setup contained an ATP-regenerating system (5 mM ATP, 1 mg/ml creatine kinase, 400 mM creatine phosphatase, 10 mM PIPES/KOH, pH 6,8, 0.2 M sorbitol), 100 nM His_6-Vam7, or 150 nM HOPS. The colorimetric substrate *p*-nitrophenolphosphate of the phosphatase Pho8 was added, and the activity was determined by absorbance measurement of the generated nitrophenol at 400 nm (Haas, 1995; LaGrassa and Ungermann, 2005).

Liposome preparation for tethering assay

Extruded liposomes were done as before (Cabrera *et al.*, 2010), with modifications. Lipid mix contained 68 mol% palmitoyl oleoyl phosphatidylcholine (POPC), 18 mol% palmitoyl oleoyl phosphatidylethanolamine (POPE), 8 mol% ergosterol, 1 mol% diacylglycerol (DAG), 1 mol% PI-3-P, 1 mol% Atto488 (purchased from AttoTec), and, where indicated, 3 mol% DOGS-NTA or compensatory amounts of POPC. Lipid films were prepared by evaporation and resuspended in HEPES/KOAc buffer (50 mM HEPES/KOH, pH 7.2, and 120 mM KOAc). After five steps of thawing and freezing in liquid nitrogen, the 2 mM liposome suspension was extruded through polycarbonate filters with a pore sizes of 100 nm using a hand extruder (Avanti Polar Lipids). The liposome radius was determined by dynamic light scattering in a DynaPro system (Wyatt Technology).

Preparation of giant unilamellar vesicles

GUVs were prepared as described (Malsam *et al.*, 2012), with some modifications. A 1 µmol amount of dried lipid mix (68.5 mol% POPC, 18 mol% POPE, 8 mol% ergosterol, 1 mol% DAG, 1 mol% PI-3-P, 0.5 mol% Atto550 [AttoTec], and 3% DOGS-NTA [or compensatory amounts of POPC]) was resolved in trehalose buffer (20 mM trehalose, 1 mM HEPES/KOH, pH 7.4, 1% glycerol [vol/vol], 1 mM DTT) for a final lipid concentration of 2 mM. Lipids were then sedimented by a centrifugation step in TLA-55 rotor (Beckman) for 2 h at 55,000 rpm. Pellets were resuspended in a total volume of 20 µl and spread as a uniform layer (diameter, ~10 mm) on the surface of ITO-coated glass slides (Nanion Technologies). The lipid suspension was dried for 12 h at low vacuum (100 mbar). An O-ring (20 × 2 mm) between two ITO slides formed the electroformation chamber, which was filled with GUV swelling buffer (240 mM sucrose, 1 mM HEPES/KOH, pH 7.4, 1 mM DTT). Electroformation was carried out for 15 h at 10 Hz and 1 V at room temperature. GUVs were collected from the slides by gentle pipetting and were ready to use for tethering assays.

Tethering assay

The assay was modified from Orr *et al.* (2015). Liposomes and GUVs were loaded with GDP- or GTP-charged Ypt7 carrying a C-terminal His_6 tag at a molar protein:lipid ratio of 1:2000. For this purpose, 7.5 µl of 2 mM liposomes or 2 mM GUVs was incubated with 0.8 µl of 10 µM GDP- or GTP-loaded Ypt7 (as described for Rab pull down) and filled up to 13.5 µl with GUV fusion buffer (135 mM NaCl, 25 mM HEPES/NaOH, pH 7.4), followed by an incubation step for 10 min at 27°C.

For GUV–liposome tethering, 0.25 mM GUVs and 0.125 mM Ypt7-loaded liposomes were incubated with HOPS, HOPS mutants, or corresponding buffer in a final volume of 20 µl. Reactions were incubated for 10 min at 27°C with gentle agitation, followed by a dilution with 80 µl of GUV fusion buffer. For liposome tethering, 0.170 mM Ypt7-loaded liposomes were incubated with indicated HOPS amounts, followed by an incubation step as described and a dilution with GUV fusion buffer.

After addition of GUV fusion buffer, 20 µl of each reaction was removed and directly transferred to a 348-well plate. The remaining 80 µl was centrifuged for 5 min at 1100 × *g* in a Swing-bucket rotor A-8-11 (Eppendorf). Tubes were removed carefully, and 20 µl from each top portion was removed and also transferred to a 384-well

plate. Atto488 fluorescence of the liposomes (emission, 501 nm; excitation, 523 nm) was measured in a SpectraMax M3 fluorescence plate reader (Molecular Devices) for 5 min at 27°C. The five readings were averaged, and the amount of tethered liposomes was calculated from the deviation in fluorescence of the two probes per sample.

Fluorescence microscopy and FM4-64 staining

For GFP microscopy and FM4-64 staining, yeast cells were grown to mid logarithmic phase (OD_{600} = 0.5) in yeast extract/peptone/dextrose (YPD) medium. Cells were pelleted for 2 min at 2000 × *g* and resuspended in 30 µl of fresh YPD medium. After incubation with 30 µM FM4-64 for 15 min at 30°C cells, were washed once with 500 µl of sterile water, followed by a second incubation step at 30°C for 30 min in 1 ml of YPD. Finally, cells were washed in SDC+ all medium and resuspended in 20 µl SDC+ all. Images were acquired with the DeltaVision Elite microscope (Applied Precision) equipped with a 100× objective (numerical aperture 1.49), a scientific complementary metal-oxide semiconductor (CMOS) camera, and filters for fluorescein isothiocyanate, tetramethylrhodamine isothiocyanate, A594, and Cy-5. Pictures were deconvolved using SoftWoRx software, version 5.9, and processed with ImageJ.

Electron microscopy and image processing

The purified samples were negatively stained adapted to the protocol as previously described (Ohi *et al.*, 2004). Briefly, a 4-µl drop of sample solution was adsorbed to a glow-discharged carbon-coated copper grid, washed with two 20-µl drops of deionized water, and stained with two 20-µl drops of freshly prepared 0.035 mg/ml uranyl formate solution. Images were collected using a Jeol JEM-1400 equipped with a LaB_6 cathode operated at 120 kV. The micrographs were taken on a CMOS camera (TVIPS TemCam F-416, 4kx4k). After manual selection of the single particles, reference-free and reference-based alignment, as well as K-means classification, were performed with EMAN2 and SPARX as described (Bröcker *et al.*, 2012).

Liposome pelleting assay

Liposomes with a diameter of 100 nm were left untreated or incubated with GDP- or GTP-charged Ypt7 carrying a C-terminal His_6-tag at a molar protein:lipid ratio of 1:2000. For this purpose, 12.5 µl of 2 mM liposomes was incubated with 1.5 µl of 10 µM precharged Ypt7 and filled up to 22.3 µl with GUV fusion buffer (135 mM NaCl, 25 mM HEPES/NaOH, pH 7.4), followed by an incubation step for 10 min at 27°C.

Were incubated 0.22 mM of these Ypt7-loaded liposomes with 227 nM HOPS or HOPS mutants in a final volume of 100 µl for 10 min at 27°C with gentle agitation. Then reactions were centrifuged (30 min, 20,000 × *g*, 4°C), the supernatants were removed, and proteins were TCA precipitated. Supernatants and pellets were resolved in SDS sample buffer, and 80% of each sample was analyzed on SDS–PAGE gels via Coomassie staining.

ACKNOWLEDGMENTS

We thank Cornelia Bröcker for support and preliminary work and Daniel Kümmel, Florian Fröhlich, and Siegfried Engelbrecht-Vandré for feedback. This work was supported by the Sonderforschungsbereich 944 (Project P11), the Deutsche Forschungsgemeinschaft (UN111/5-4 to C.U. and RA1781/2-4 to S.R.), and the Hans-Mühlenhoff Foundation (to C.U.).

REFERENCES

Anand VC, Daboussi L, Lorenz TC, Payne GS (2009). Genome-wide analysis of AP-3-dependent protein transport in yeast. Mol Biol Cell 20, 1592–1604.

Auffarth K, Arlt H, Lachmann J, Cabrera M, Ungermann C (2014). Tracking of the dynamic localization of the Rab-specific HOPS subunits reveal their distinct interaction with Ypt7 and vacuoles. Cellularlogistics 4, e29191.

Baker RW, Jeffrey PD, Zick M, Phillips BP, Wickner WT, Hughson FM (2015). A direct role for the Sec 1/Munc18-family protein Vps33 as a template for SNARE assembly. Science 349, 1111–1114.

Balderhaar HJK, Lachmann J, Yavavli E, Bröcker C, Lürick A, Ungermann C (2013). The CORVET complex promotes tethering and fusion of Rab5/Vps21-positive membranes. Proc Natl Acad Sci USA 110, 3823–3828.

Balderhaar HJK, Ungermann C (2013). CORVET and HOPS tethering complexes - coordinators of endosome and lysosome fusion. J Cell Sci 126, 1307–1316.

Barr FA (2013). Review series: Rab GTPases and membrane identity: causal or inconsequential? J Cell Biol 202, 191–199.

Brachmann C, Davies A, Cost G, Caputo E, Li J, Hieter P, Boeke J (1998). Designer deletion strains derived from Saccharomyces cerevisiae S288C: a useful set of strains and plasmids for PCR-mediated gene disruption and other applications. Yeast 14, 115–132.

Brett CL, Plemel RL, Lobingier BT, Lobinger BT, Vignali M, Fields S, Merz AJ (2008). Efficient termination of vacuolar Rab GTPase signaling requires coordinated action by a GAP and a protein kinase. J Cell Biol 182, 1141–1151.

Bröcker C, Kuhlee A, Gatsogiannis C, Kleine Balderhaar HJ, Hönscher C, Engelbrecht-Vandré S, Ungermann C, Raunser S (2012). Molecular architecture of the multisubunit homotypic fusion and vacuole protein sorting (HOPS) tethering complex. Proc Natl Acad Sci USA 109, 1991–1996.

Burguete A, Fenn T, Brunger A, Pfeffer S (2008). Rab and Arl GTPase family members cooperate in the localization of the golgin GCC185. Cell 132, 286–298.

Cabrera M, Langemeyer L, Mari M, Rethmeier R, Orban I, Perz A, Bröcker C, Griffith J, Klose D, Steinhoff HJ, *et al.* (2010). Phosphorylation of a membrane curvature-sensing motif switches function of the HOPS subunit Vps41 in membrane tethering. J Cell Biol 191, 845–859.

Cabrera M, Nordmann M, Perz A, Schmedt D, Gerondopoulos A, Barr F, Piehler J, Engelbrecht-Vandré S, Ungermann C (2014). The Mon1-Ccz1 GEF activates the Rab7 GTPase Ypt7 via a longin-fold-Rab interface and association with PI3P-positive membranes. J Cell Sci 127, 1043–1051.

Cabrera M, Ostrowicz CW, Mari M, LaGrassa TJ, Reggiori F, Ungermann C (2009). Vps41 phosphorylation and the Rab Ypt7 control the targeting of the HOPS complex to endosome-vacuole fusion sites. Mol Biol Cell 20, 1937–1948.

Cao X, Ballew N, Barlowe C (1998). Initial docking of ER-derived vesicles requires Uso1p and Ypt1p but is independent of SNARE proteins. EMBO J 17, 2156–2165.

Cao X, Barlowe C (2000). Asymmetric requirements for a Rab GTPase and SNARE proteins in fusion of COPII vesicles with acceptor membranes. J Cell Biol 149, 55–66.

Cheung P-YP, Limouse C, Mabuchi H, Pfeffer SR (2015). Protein flexibility is required for vesicle tethering at the Golgi. Elife 4, e12790.

Collins KM, Thorngren NL, Fratti RA, Wickner WT (2005). Sec 17p and HOPS, in distinct SNARE complexes, mediate SNARE complex disruption or assembly for fusion. EMBO J 24, 1775–1786.

Drin G, Morello V, Casella J-F, Gounon P, Antonny B (2008). Asymmetric tethering of flat and curved lipid membranes by a golgin. Science 320, 670–673.

Eathiraj S, Pan X, Ritacco C, Lambright DG (2005). Structural basis of family-wide Rab GTPase recognition by rabenosyn-5. Nature 436, 415–419.

Haas A (1995). A quantitative assay to measure homotypic vacuole fusion in vitro. Methods Cell Sci 17, 283–294.

Hickey CM, Wickner W (2010). HOPS initiates vacuole docking by tethering membranes before trans-SNARE complex assembly. Mol Biol Cell 21, 2297–2305.

Ho R, Stroupe C (2015). The HOPS/class C Vps complex tethers membranes by binding to one Rab GTPase in each apposed membrane. Mol Biol Cell 26, 2655–2663.

Ho R, Stroupe C (2016). The HOPS/Class C Vps complex tethers high-curvature membranes via a direct protein-membrane interaction. Traffic 17, 1078–1090.

Jun Y, Thorngren N, Starai VJ, Fratti RA, Collins K, Wickner W (2006). Reversible, cooperative reactions of yeast vacuole docking. EMBO J 25, 5260–5269.
Kümmel D, Ungermann C (2014). Principles of membrane tethering and fusion in endosome and lysosome biogenesis. Curr Opin Cell Biol 29C, 61–66.
LaGrassa TJ, Ungermann C (2005). The vacuolar kinase Yck3 maintains organelle fragmentation by regulating the HOPS tethering complex. J Cell Biol 168, 401–414.
Lobingier BT, Nickerson DP, Lo SY, Merz AJ (2014). SM proteins Sly1 and Vps33 coassemble with Sec 17 and SNARE complexes to oppose SNARE disassembly by Sec 18. Elife 3, e02272.
Lürick A, Kuhlee A, Bröcker C, Kümmel D, Raunser S, Ungermann C (2015). The HABC domain of the SNARE Vam3 interacts with the HOPS tethering complex to facilitate vacuole fusion. J Biol Chem 290, 5405–5413.
Malsam J, Parisotto D, Bharat TAM, Scheutzow A, Krause JM, Briggs JAG, Söllner TH (2012). Complexin arrests a pool of docked vesicles for fast Ca2+-dependent release. EMBO J 31, 3270–3281.
Mishra A, Eathiraj S, Corvera S, Lambright DG (2010). Structural basis for Rab GTPase recognition and endosome tethering by the C2H2 zinc finger of Early Endosomal Autoantigen 1 (EEA1). Proc Natl Acad Sci USA 107, 10866–10871.
Morgera F, Sallah MR, Dubuke ML, Gandhi P, Brewer DN, Carr CM, Munson M (2011). Regulation of exocytosis by the exocyst subunit Sec6 and the SM protein Sec1. Mol Biol Cell 23, 337–346.
Murray DH, Jahnel M, Lauer J, Avellaneda MJ, Brouilly N, Cezanne A, Morales-Navarrete H, Perini ED, Ferguson C, Lupas AN, *et al.* (2016). An endosomal tether undergoes an entropic collapse to bring vesicles together. Nature 537, 107–111.
Nordmann M, Cabrera M, Perz A, Bröcker C, Ostrowicz CW, Engelbrecht-Vandré S, Ungermann C (2010). The Mon1-Ccz1 complex is the GEF of the late endosomal Rab7 homolog Ypt7. Curr Biol 20, 1654–1659.
Ohi M, Li Y, Cheng Y, Walz T (2004). Negative staining and image classification—powerful tools in modern electron microscopy. Biol Proced Online 6, 23–34.
Ohya T, Miaczynska M, Coskun Ü, Lommer B, Runge A, Drechsel D, Kalaidzidis Y, Zerial M (2009). Reconstitution of Rab- and SNARE-dependent membrane fusion by synthetic endosomes. Nature 459, 1091–1097.
Orr A, Wickner W, Rusin SF, Kettenbach AN, Zick M (2015). Yeast vacuolar HOPS, regulated by its kinase, exploits affinities for acidic lipids and Rab:GTP for membrane binding and to catalyze tethering and fusion. Mol Biol Cell 26, 305–315.
Ostrowicz CW, Bröcker C, Ahnert F, Nordmann M, Lachmann J, Peplowska K, Perz A, Auffarth K, Engelbrecht-Vandré S, Ungermann C (2010). Defined subunit arrangement and rab interactions are required for functionality of the HOPS tethering complex. Traffic 11, 1334–1346.
Peplowska K, Markgraf DF, Ostrowicz CW, Bange G, Ungermann C (2007). The CORVET tethering complex interacts with the yeast Rab5 homolog Vps21 and is involved in endo-lysosomal biogenesis. Dev Cell 12, 739–750.
Plemel RL, Lobingier BT, Brett CL, Angers CG, Nickerson DP, Paulsel A, Sprague D, Merz AJ (2011). Subunit organization and Rab interactions of Vps-C protein complexes that control endolysosomal membrane traffic. Mol Biol Cell 22, 1353–1363.
Rai A, Oprisko A, Campos J, Fu Y, Friese T, Itzen A, Goody RS, Gazdag EM, Müller MP (2016). bMERB domains are bivalent Rab8 family effectors evolved by gene duplication. Elife 5, e18675.
Starai VJ, Hickey CM, Wickner W (2008). HOPS proofreads the trans-SNARE complex for yeast vacuole fusion. Mol Biol Cell 19, 2500–2508.
Stroupe C, Collins KM, Fratti RA, Wickner W (2006). Purification of active HOPS complex reveals its affinities for phosphoinositides and the SNARE Vam7p. EMBO J 25, 1579–1589.
Stroupe C, Hickey CM, Mima J, Burfeind AS, Wickner W (2009). Minimal membrane docking requirements revealed by reconstitution of Rab GTPase-dependent membrane fusion from purified components. Proc Natl Acad Sci USA 106, 17626–17633.
Takamori S, Holt M, Stenius K, Lemke E, Gronborg M, Riedel D, Urlaub H, Schenck S, Brugger B, Ringler P, *et al.* (2006). Molecular anatomy of a trafficking organelle. Cell 127, 831–846.
Tall G, Hama H, DeWald D, Horazdovsky B (1999). The phosphatidylinositol 3-phosphate binding protein Vac1p interacts with a Rab GTPase and a Sec1p homologue to facilitate vesicle-mediated vacuolar protein sorting. Mol Biol Cell 10, 1873–1889.
van der Kant R, Jonker CT, Wijdeven RH, Bakker J, Janssen L, Klumperman J, Neefjes J (2015). Characterization of the mammalian CORVET and HOPS complexes and their modular restructuring for endosome specificity. J Biol Chem 290, 30280–30290.
Vetter M, Stehle R, Basquin C, Lorentzen E (2015). Structure of Rab11–FIP3– Rabin8 reveals simultaneous binding of FIP3 and Rabin8 effectors to Rab11. Nat Struct Mol Biol 22, 695–702.
Wang L, Merz A, Collins K, Wickner W (2003). Hierarchy of protein assembly at the vertex ring domain for yeast vacuole docking and fusion. J Cell Biol 160, 365–374.
Wong M, Munro S (2014). The specificity of vesicle traffic to the Golgi is encoded in the golgin coiled-coil proteins. Science 346, 1256898.
Wurmser AE, Sato TK, Emr SD (2000). New component of the vacuolar class C-Vps complex couples nucleotide exchange on the Ypt7 GTPase to SNARE-dependent docking and fusion. J Cell Biol 151, 551–562.
Zick M, Wickner W (2012). Phosphorylation of the effector complex HOPS by the vacuolar kinase Yck3p confers Rab nucleotide specificity for vacuole docking and fusion. Mol Biol Cell 23, 3429–3437.
Zick M, Wickner WT (2014). A distinct tethering step is vital for vacuole membrane fusion. Elife 3, e03251.